Defect structure and formation of defect complexes in Cu2+-modified metal oxides derived from a spin-Hamiltonian parameter analysis

Rüdiger Eichel

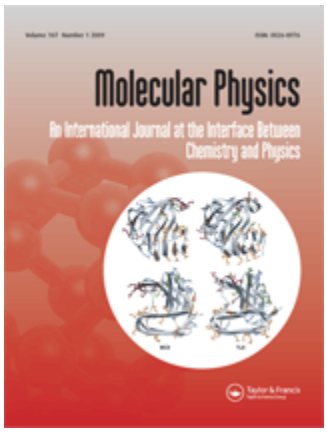

Defect structure and formation of defect complexes in Cu2+-modified metal oxides derived from a spin-Hamiltonian parameter analysis

Journal:	*Molecular Physics*
Manuscript ID:	TMPH-2009-0093.R1
Manuscript Type:	Full Paper
Date Submitted by the Author:	10-Apr-2009
Complete List of Authors:	Eichel, Rüdiger; Universität Freiburg, Physikalische Chemie I
Keywords:	EPR, spin Hamiltonian, copper functional center, defect structure, ferroelectrics
Note: The following files were submitted by the author for peer review, but cannot be converted to PDF. You must view these files (e.g. movies) online.	
paper09_resubmitted.tex	

Defect structure and formation of defect complexes in Cu^{2+}-modified metal oxides derived from a spin-Hamiltonian parameter analysis

Rüdiger-A. Eichel,[1,*] Michael D. Drahus,[1] Peter Jakes,[1] Ebru Erünal,[1]
Emre Erdem,[1] S.K.S. Parashar,[2] Hans Kungl,[3] and Michael J. Hoffmann[3]

[1] *Universität Freiburg, Institut für Physikalische Chemie I, Albertstr. 21, D-79104 Freiburg, Germany*
[2] *Department of Physics and Meteorology, Indian Institute of Technology, Kharagpur - 721302, India*
[3] *Institute of Ceramics in Mechanical Engineering, University of Karlsruhe, D-76131 Karlsruhe, Germany*

(Dated: April 10, 2009)

The nearest neighbor oxygen octahedron about copper functional centers in metal oxides has been systematically studied by means of electron paramagnetic resonance (EPR) spectroscopy. In particular, the determined $g_{\parallel,zz}$ and $A^{\mathrm{Cu}}_{\parallel,zz}$ spin-Hamiltonian parameters were analyzed, finding linear dependences as function of chemical bonding and local distortion of the oxygen octahedron. Moreover, through the introduction of a dimensionless *coordination parameter* ξ, different defect structures with respect to the number of coordinated oxygen vacancies may be distinguished. This allows for a distinct assignment of defect complexes between the copper functional center with one or two oxygen vacancies.

Keywords: ferroelectrics, defect structure, copper doping, oxygen vacancy, defect dipole

INTRODUCTION

An important issue in the class of ferroelectric materials is the control of defect structure by means of aliovalent doping in order to tailor device properties for specific applications [1]. Whereas in so-termed '*hard*' materials, relatively low dielectric constants or high coercive fields are obtained, '*soft*' compounds show an increased dielectric constant, high dielectric loss or low coercive field. For PZT ($Pb[Zr_xTi_{1-x}]O_3$), it is well established that acceptor-type dopants form defect dipoles with charge-compensating oxygen vacancies [2], such as $(Ni''_{Ti} - V_O^{\bullet\bullet})^{\times}$ [3], $(Cu''_{Ti} - V_O^{\bullet\bullet})^{\times}$ [4], $(Fe'_{Zr,Ti} - V_O^{\bullet\bullet})^{\bullet}$ [5, 6] or $(Mn''_{Ti} - V_O^{\bullet\bullet})^{\times}$ [7]. However, excess doping of acceptor-type ions over the solubility limit may result in the formation of secondary phases [8]. On the other hand, donor-type functional centers rather occur as 'isolated' centers ($Gd^{\bullet}_{Pb}$) and the corresponding lead vacancies (V''_{Pb}) generated for reason of charge compensation are located in distant coordination spheres [9]. When considering lattice vacancies, in particular the role of oxygen vacancies is currently controversially discussed with respect to dynamic phenomena such as *ferroelectric aging* [10, 11] or *electrical fatigue* [12–15].

The *method-of-choice* to characterize paramagnetic dopants is provided by electron paramagnetic resonance (EPR) spectroscopy [16, 17]. In particular, recent methododical advances concerning the use of high frequencies [18–21] and pulsed microwave fields [4, 22, 23] have allowed for an accurate determination of spin-Hamiltonian parameters. However, as compared to the high-spin ions Fe^{3+} and Mn^{2+}, both of which have a $3d^5$ electronic configuration and thus $S = \frac{5}{2}$, Cu^{2+} has only one unpaired electron ($3d^9$, $S = \frac{1}{2}$), for which reason the electron fine-structure interaction that probes the electrical field gradient at the Cu^{2+}-site vanishes. Consequently, there is no means to transfer the determined spin-Hamiltonian parameters into defect-structural information by applying the Newman superposition model [24]. In order to circumvent this disadvantage, in conjunction with density functional theoretic calculations, the orientation-dependence of the transferred spin-density obtained by hyperfine sublevel correlation experiments (HYSCORE) has recently been analyzed proving the existence of a $(Cu''_{Ti} - V_O^{\bullet\bullet})^{\times}$ defect dipole [4].

We here aim to present a systematic empirical and experimentally much simpler approach in relating the size of spin-Hamiltonian parameters to different defect-structural arrangements with particular focus to elucidate the impact of nearest neighbor lattice vacancies on the EPR spin-Hamiltonian parameters.

THEORY

The spin Hamiltonian for an unpaired $3d^9$ electron with spin $S = \frac{1}{2}$ can be written as [25]

$$\mathcal{H} = \beta_e \mathbf{B_0} \cdot \mathbf{g} \cdot \mathbf{S} - \beta_n g_n \mathbf{B_0} \cdot \mathbf{I} + \mathbf{S} \cdot \mathbf{A} \cdot \mathbf{I} \qquad (1)$$

where g_n is the corresponding nuclear g-factor and β_e and β_n are the Bohr and nuclear magnetons, respectively. The first and second terms represent the electronic and nuclear Zeeman interactions, respectively, where $\mathbf{B_0}$ denotes the external field, given in the principal axes system of the $\mathbf{g}$-matrix. The last term is due to the copper hyperfine interaction with $I^{\mathrm{Cu}} = \frac{3}{2}$ for both copper isotopes with natural abundances ^{63}Cu: 69.09% and ^{65}Cu: 30.91%.

Generally, the hyperfine tensor $\mathbf{A}$ has contributions from the *isotropic* Fermi-contact interaction $a_{\mathrm{iso}}\mathbf{S} \cdot \mathbf{I}$ and

the *anisotropic* electron-nuclear dipole-dipole coupling $\mathbf{S}\cdot\mathbf{A}'\cdot\mathbf{I}$, such that

$$\mathbf{A} = a_{\mathrm{iso}}\mathbf{1} + \mathbf{A}' \tag{2}$$

The Fermi-contact interaction is parametrized by the isotropic hyperfine coupling constant

$$a_{\mathrm{iso}} = \frac{2\mu_0}{3\hbar} g_e \beta_e g_n \beta_n \left|\psi_0(r=0)\right|^2 \tag{3}$$

where $|\psi_0(r=0)|^2$ is the electron spin density at the corresponding nucleus. Generally, a_{iso} is induced by unpaired electrons in *s*-orbitals, which are centered at the nucleus. However, isotropic hyperfine interaction may also be significant when the unpaired electron resides in a *p*-, *d*- or *f*-orbital. The spin density at the nucleus is then induced by configuration interactions or spin-polarization mechanisms [26, 27].

The energy levels for a divalent copper functional center coordinated by an oxygen octahedron in a solid may be described in terms of a crystal-field model [28]. Generally, EPR is performed in the ground state, which is $^2D_{5/2}$ for Cu^{2+}. In a cubic octahedral crystal field, the degeneracy of the $^2D_{5/2}$ ground state is partially lifted into a doublet (^2E_g) lying lowest and a triplet ($^2T_{2g}$), as schematically illustrated in figure 1. If the crystal symmetry is tetragonally (axially) distorted, the triplet splits into a singlet ($^2B_{2g}$) with the atomic orbital $|xy\rangle$ and a doublet (^2E_g) with orbitals $|yz\rangle$ and $|zx\rangle$, respectively. Furthermore, the doublet state is split into two non-degenerate $^2B_{1g}$ and $^2A_{1g}$ levels with the atomic orbitals $|x^2-y^2\rangle$ and $|3z^2-r^2\rangle$, respectively. The ordering of these levels depends upon the tetragonal crystal distortion being either an elongation or a compression. A further lowering of crystal symmetry from tetragonal to rhombic, lifts the remaining degeneracy of the ^2E_g level.

In tetragonal symmetry, the principal values of the *g*-matrix and the $\mathbf{A^{Cu}}$-hyperfine tensor in its eigen-system ($g_\parallel$, $g_\perp$, $A_\parallel^{\mathrm{Cu}}$, $A_\perp^{\mathrm{Cu}}$) may be given as a function of the crystal field [25]. Using second-order perturbation theory, the principal values of the **g**-matrix are as follows

$$g_\parallel = g_e\left[1 - \frac{8\lambda}{\Delta_0}\right] \tag{4}$$

$$g_\perp = g_e\left[1 - \frac{2\lambda}{\Delta_1}\right] \tag{5}$$

where $g_e = 2.0023$ is the free electron *g*-value, λ is the spin-orbit coupling constant, and $\Delta_{0,1}$ the energy splittings of the Cu^{2+} ion in a tetragonally distorted octahedral crystal field (cf. figure 1). Typically, an optical absorption of $\Delta = 12300\ \mathrm{cm}^{-1}$ may be taken as a mean value for $\Delta_{0,1}$ and $\lambda = -710\ \mathrm{cm}^{-1}$ is considerably smaller than the free-ion value ($-830\ \mathrm{cm}^{-1}$) owing to an 'orbital reduction' attributed to covalent bonding to the surrounding ions. Consequently, typical values of $\frac{\lambda}{\Delta}$ range from -0.05 to -0.1. The deviation from $g_\parallel$, $g_\perp$ according to equations (4,5) from g_e may be explained by spin-orbit coupling, where some of the excited states are mixed to the ground state, resulting in a *g*-anisotropy ($g_\parallel \neq g_\perp$) and particularly in *g*-values larger than g_e in case of Cu^{2+}. The closer the excited states to the ground state and the larger the spin-orbit coupling, the larger the deviation of the *g* principal values from g_e.

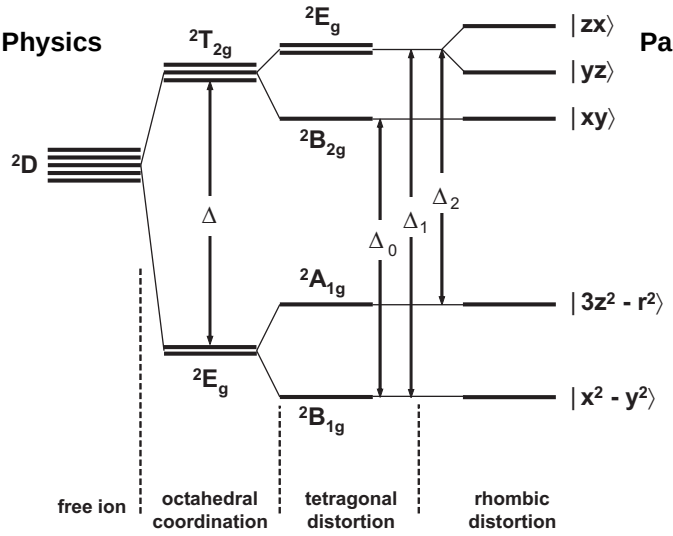

FIG. 1: Schematic representation of the orbital energy levels for Cu^{2+} in a crystal field of octahedral symmetry with tetragonal and rhombic distortion. The cubic (Δ) and tetragonal ($\Delta_{0,1,2}$) field splittings are indicated.

For the $\mathbf{A^{Cu}}$-tensor, the principal values are given by

$$A_\parallel^{\mathrm{Cu}} = P\left[-\kappa - \frac{4}{7} - \frac{6\lambda}{7\Delta_1} - \frac{8\lambda}{\Delta_0}\right] \tag{6}$$

$$A_\perp^{\mathrm{Cu}} = P\left[-\kappa + \frac{2}{7} - \frac{11\lambda}{7\Delta_1}\right] \tag{7}$$

where $P = 2\gamma\beta_e\beta_n\langle r^{-3}_{\mathrm{Cu}^{2+}}\rangle$, and κ is a core-polarization parameter that takes into account the spin density at the copper nucleus. Typical values are $\langle r^{-3}\rangle = 6.3$ a.u. and $\kappa = 0.32$. The terms of order $\frac{\lambda}{\Delta}$ in equations (6,7) are partly due to residual orbital contribution and partly owing to the admixture of higher states by spin-orbit coupling.

RESULTS AND DISCUSSION

In order to systematically study the principal impact of the first coordination sphere on the EPR spin-Hamiltonian parameters, Cu^{2+} in different oxygen coordination - i.e. differently distorted or truncated oxygen octahedra - was studied. The corresponding X-band (9.4 GHz) EPR spectra are shown in figure 2. All spectra can be described by *g*-matrices of axial or rhombic symmetry

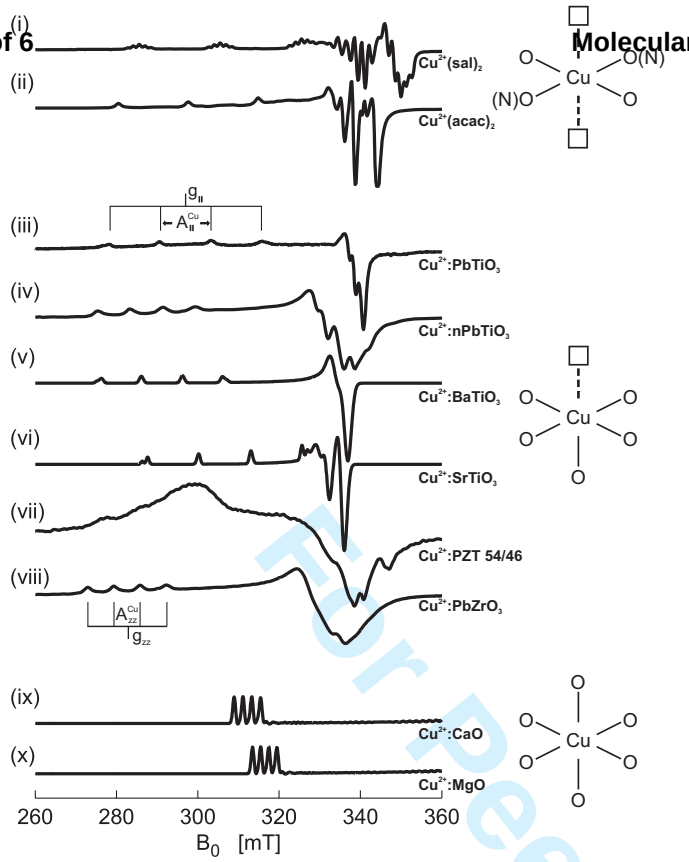

FIG. 2: Representative X-band (9.4 GHz) EPR-spectra for Cu^{2+} in different oxygen coordinations. (i,ii) - CuO_4 coordination for the square-planar Cu(II)(sal)$_2$ (i), and Cu(II)(acac)$_2$ (ii) complexes, being representative for a pseudo ($V_O^{\bullet\bullet} - Cu - V_O^{\bullet\bullet}$) defect complex. (iii-viii) - CuO_5 coordination for the aliovalently Cu^{2+}-doped $A^{2+}B^{4+}O_3^{2-}$ compounds Cu^{2+}:$PbTiO_3$ (iii), nano-sized Cu^{2+}:$PbTiO_3$ (iv), Cu^{2+}:$BaTiO_3$ (v), Cu^{2+}:$SrTiO_3$ (vi), Cu^{2+}:PZT 54/46 (vii), and $Cu^{2+}PbZrO_3$ (viii). For these materials, $(Cu''_{Zr,Ti} - V_O^{\bullet\bullet})^{\times}$ defect dipoles are formed for reason of charge compensation. (ix,x) - CuO_6 coordination for the isovalently Cu^{2+} substituted Cu^{2+}:CaO (ix), and Cu^{2+}:MgO (x) compounds. Two representative stick spectra indicate the quartet ^{63}Cu-hyperfine pattern for the $g_{\parallel,zz}$-orientations. The three different copper coordinations, CuO_x, are schematically illustrated where the open squares indicate the positions of the oxygen vacancies.

with $g_\parallel > g_\perp > g_e$ and $g_{zz} > g_{yy}, g_{xx} > g_e$, respectively. Moreover, a nicely resolved quartet in the $g_{\parallel,zz}$-region owing to the $A^{Cu}_{\parallel,zz}$-copper hyperfine splitting is observed.

The ordering of the observed g-values ($g_\parallel > g_\perp$) is characteristic for octahedrally coordinated Cu^{2+} centers, where the octahedron is elongated by a tetragonal distortion along the z-axis [25]. It can be explained in terms of a five-fold orbital degeneracy of the $3d^9$ ion that is split in the presence of an octahedral crystal field into a triplet ($^2T_{2g}$) and a doublet (^2E_g), with the latter lying lowest (cf. figure 1). A tetragonal distortion, caused by the crystal field and the Jahn-Teller effect, splits the ^2E_g levels further, resulting in an orbital-singlet $d_{x^2-y^2}$ ground state.

Variations in the observed EPR spectra are mainly due to differences in the first coordination sphere about the copper functional center, namely (1) - the nature of the chemical bonding of the copper with the nearest neighbor oxygens, (2) - the crystal field at the copper site as a function of lattice distortion, and (3) - the possible association to oxygen vacancies ($V_O^{\bullet\bullet}$).

Concerning the nature of chemical bonding, Cu^{2+}:$PbTiO_3$ [4, 20, 29, 30] with strong covalent bonding [31–34] may be compared with Cu^{2+}:$PbZrO_3$ [20] that is representative for ionic bonding [34, 35], as illustrated in figure 2(iii,viii). The most pronounced variation is observed for the $g_{\parallel,zz}$ and $A^{Cu}_{\parallel,zz}$-values; whereas $g_{\parallel,zz}$ decreases, $A^{Cu}_{\parallel,zz}$ increases for stronger covalent bonding. This observation supports a general relation for octahedrally coordinated copper compounds after which $g_{iso} = \frac{2g_\perp + g_\parallel}{3}$ decreases and $a^{Cu}_{iso} = \frac{2A^{Cu}_\perp + A^{Cu}_\parallel}{3}$ increases as a function of the covalent character of a chemical bond [36]. This relation is due to the fact that the g-values are sensitive to a change in the Cu^{2+}-O^{2-} in-plane π-bonding [37, 38], which in turn is due to the Zr^{4+}-O^{2-} bonding being more polar (ionic) than the Ti^{4+}-O^{2-} bonding because of electro-negativity differences. Furthermore, for ionic bonding, more spin density is transferred to neighboring oxygen ions, reducing the remaining spin density at the copper nucleus that in turn occurs as reduced (isotropic) copper hyperfine coupling in the EPR spectrum.

When regarding technologically relevant copper-modified PZT 54/46 (cf. figure 2(vii)) with a morphotropic-phase boundary composition, the resonances are considerably broadened as compared to the other spectra. This is owing to the fact that a solid solution of at least three different crystal structures is present. For all three copper centers intermediate $g_{\parallel,zz}$ and $A^{Cu}_{\parallel,zz}$-values in the intervals spanned by the extreme values $[g^{PT}_\parallel, g^{PZ}_{zz}]$ and $[A^{Cu:PT}_\parallel, A^{Cu:PZ}_{zz}]$, respectively, are found [18, 22].

In order to study the effect of the crystal field on the copper spin-Hamiltonian values, two tetragonal Cu^{2+}:$PbTiO_3$ compounds with varying c/a-ratio of the lattice parameters are compared. The reduction in c/a-ratio is achieved by comparing '*bulk*' Cu^{2+}:$PbTiO_3$ ($\frac{c}{a} = 1.063$, figure 2(iii)) with a Cu^{2+}:$PbTiO_3$ compound with mean particle size in the nm range ($\frac{c}{a} \approx 1.05$, figure 2(iv)) [47]. Generally, a continuous trend toward larger $g_\parallel$ and smaller $A^{Cu}_\parallel$ for decreasing c/a-ratio is observed.

For further compounds of $A^{2+}B^{4+}O_3^{2-}$ composition, such as and Cu^{2+}:$BaTiO_3$ (figure 2(v)) [39–41] and Cu^{2+}:$SrTiO_3$ (figure 2(vi)), a more complex variation of $g_\parallel$ and $A^{Cu}_\parallel$ is observed. This is owing to the fact that for these materials simultaneously the nature of chemical

bonding and the crystal field are changed.

The most important impact of defect structure on the spin-Hamiltonian parameters is expected in terms of associated lattice vacancies. These are generated when doping with aliovalent Cu^{2+} that necessitates the formation of oxygen vacancies ($V_O^{\bullet\bullet}$) for reasons of charge compensation [16, 17]. Recently, it has been shown that for PZT compounds the corresponding oxygen vacancy is created in the first coordination sphere of the copper functional center, resulting in an $(Cu''_{Zr,Ti} - V_O^{\bullet\bullet})^{\times}$ defect dipole [4, 22, 48]. In order to compare this situation to Cu^{2+} in a complete oxygen octahedron, Cu^{2+}-modified compounds are studied where copper isovalently substitutes for a divalent ion, such that no charge compensation by means of oxygen vacancies is necessary. This effect is illustrated by a comparison with copper-doped CaO and MgO ($Cu^{\times}_{Ca,Mg}$), as shown in figure 2(ix,x) for numerically simulated spectra [49, 50]. Despite the cubic crystal symmetry axially symmetric EPR spectra are observed, which is owing to the Jahn-Teller effect [49–52]. As compared to the $(Cu''_{Zr,Ti} - V_O^{\bullet\bullet})^{\times}$ defect dipoles, a drastic reduction in $A_{\parallel}^{Cu}$ is observed, whereas the $g_{\parallel}$-value is only slightly affected. In analogy to the impact of ionicity, the increase in (isotropic) copper hyperfine coupling can be attributed to an additional oxygen ion in the first coordination sphere to which spin density is transferred, reducing the remaining spin density at the copper nucleus. This observation corresponds well with an expectation taking into account an enhanced core-polarization κ owing to a missing oxygen ion in the octahedron, which reduces the value for $A_{\parallel}^{Cu}$ according to equation (6).

The results obtained with respect to the perovskite structure so far, are representative for compounds with tetravalent B-site ($A^{2+}B^{4+}O_3^{2-}$). However, in recently investigated 'lead-free' ferroelectrics, the B-site may have a different charge state; pentavalent ($A^{+}B^{5+}O_3^{2-}$) for $[K_yNa_{1-y}]NbO_3$(KNN) compositions and trivalent ($A^{3+}B^{3+}O_3^{2-}$) for Bi-containing ferroelectrics. Particularly for KNN with pentavalent B-site, defects of the type $(V_O^{\bullet\bullet} - Cu'''_{Nb} - V_O^{\bullet\bullet})^{\bullet}$ with two simultaneously coordinated oxygen vacancies become energetically conceivable. In order to account for this situation, inorganic copper complexes with square-planar oxygen coordination are regarded as model-type substances. Owing to the square-planar oxygen coordination, such compounds may serve as model substance with a pseudo $(V_O - Cu - V_O)$ defect complex. The corresponding EPR spectra of bis(salicylaldoximato)Cu(II), $Cu(sal)_2$, diluted into a $Ni(sal)_2$ powder [42–44] and bis(acetylacetonato)Cu(II), $Cu(acac)_2$, diluted into a $Pd(acac)_2$ matrix [45, 46] are depicted in figure 2(i,ii). For these compounds, a considerably increased $A_{\parallel}^{Cu}$-hyperfine splitting and slightly reduced $g_{\parallel}$-value are observed. This continues the trend observed for the formation of one oxygen vacancy in the first coordination sphere, where the increased hyperfine splitting is explained by reduced transferred spin density to neighboring oxygens and enhanced core-polarization κ reducing $A_{\parallel}^{Cu}$ according to equation (6).

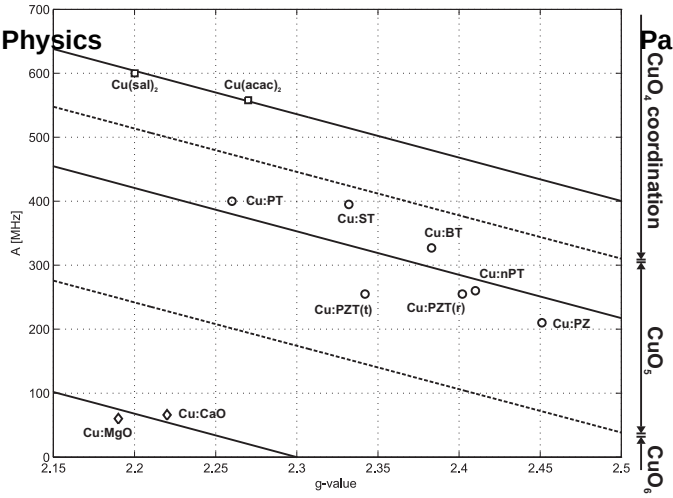

FIG. 3: Linear dependencies of $g_{\parallel,zz}$ versus ${}^{63}A_{\parallel,zz}^{Cu}$ spin-Hamiltonian parameters for varying oxygen coordinations about Cu^{2+} centers with indicated defect structure, i.e. number of associated oxygen vacancies. The solid lines represent the linear dependency according to equation (8) for a given defect structure. Top - formation of $(V_O^{\bullet\bullet} - Cu^{2+} - V_O^{\bullet\bullet})$ defect complexes (CuO_4 coordination), center - formation of $(V_O^{\bullet\bullet} - Cu^{2+})$ defect dipoles (CuO_5 coordination), bottom - 'isolated' Cu^{2+} functional center in complete oxygen octahedra (CuO_6 coordination). The dashed lines tentatively mark the separation between the regions for the different defect structures.

Principally, when regarding ionic sizes, copper could also be substituted onto the twelve-fold coordinated perovskite A-site. Depending on the host system, the corresponding functional centers would range from donor-type $Cu^{\bullet}_{K,Na}$ in KNN over isovalently substituted $Cu^{\times}_{Pb}$ in PZT to acceptor-type Cu'_{Bi} for Bi-containing compounds. However, a twelve-fold coordinated Cu^{2+}-center has never been reported in literature so far [53–57], for which reason this situation is ruled out. Hypothetically, the trend observed so far with increasing $A_{\parallel}^{Cu}$ and decreasing $g_{\parallel}$ as a function of the number of coordinated oxygen ions, allows for a rough estimation of $A_{\parallel}^{Cu} < 50$ MHz and $g_{\parallel} > 2.5$ for such a center.

Generally, when regarding octahedral oxygen coordination about an Cu^{2+}-ion, four of the ligand oxygens typically are disposed in an approximate plane including the copper ion. These oxygen ions are rather close to the copper and strongly bonded. The remaining two ligand oxygens are arranged on a line perpendicular to that plane, and are usually more weakly bound to the copper than those in the plane. Spectroscopically, this arrangement defines the orientation of the spin-Hamiltonian g-matrix, such that $g_{\perp}$ (g_{xx}, g_{yy}) lie in the plane and $g_{\parallel}$

TABLE I: Experimentally obtained *coordination parameter* ξ for Cu^{2+} in octahedral symmetry with varying number of associated oxygen vacancies.

defect structure	coordination parameter
Cu^{2+}	$\xi_{CuO_6} = 3.09$
$(Cu^{2+} - V_O^{\bullet\bullet})$	$\xi_{CuO_5} = 2.82$
$(V_O^{\bullet\bullet} - Cu^{2+} - V_O^{\bullet\bullet})$	$\xi_{CuO_4} = 2.30$

(g_{zz}) are perpendicular to the plane. Owing to the different strengths of chemical bonding in the plane and perpendicular to it, an oxygen vacancy will rather be coordinated along $g_\parallel$ than $g_\perp$. Consequently, when studying effects of $V_O^{\bullet\bullet}$-coordination, a relevant set of spin-Hamiltonian parameters is ($g_\parallel$, $A_\parallel^{Cu}$). Obviously, these are also much better resolved in the EPR spectra than ($g_\perp$, $A_\perp$). For this reason, $g_\parallel$ is plotted against $A_\parallel^{Cu}$ as depicted in figure 3. In this representation, linear dependencies of the form

$$A_\parallel^{Cu} = 2\pi P(\xi - g_\parallel) \tag{8}$$

are observed, where different defect structures in terms of complete oxygen octahedron versus association of various numbers of oxygen vacancies are described by a dimensionless *coordination parameter* ξ. The corresponding values of ξ are summarized in table I. Neglecting the variation of κ as a function of the number of coordinated oxygen vacancies, the linear dependency (8) emerges in first approximation from equations (4,6). The here developed analysis is not restricted to ferroelectrics, but may also be extended to study the defect structure in other copper-doped metal oxides.

A similar representation than the one of figure 3 has already been introduced in *life-science* by means of so-termed *Peisach-Blumberg* plots [58] in order to distinguish between different chemical environments. Similar to the observation found here, a systematic variation in the spin-Hamiltonian parameters depending on the overall charge of the system and the nature of ligand atoms (O, N, S) was observed.

CONCLUSION

In summary, an empirical relationship between the $g_\parallel$ and $A_\parallel^{Cu}$ spin-Hamiltonian parameters as obtained from EPR is presented that allows for a direct assignment of defect structure with respect to the existence of 'isolated' Cu_B centers in a complete oxygen octahedron or the formation of $(V_O^{\bullet\bullet} - Cu_B)$ and $(V_O^{\bullet\bullet} - Cu_B - V_O^{\bullet\bullet})$ defect complexes with electric and elastic properties in Cu^{2+}-modified ABO_3 perovskite oxides.

ACKNOWLEDGMENTS

It is a pleasure to acknowledge the continuous support of Professor Stefan Weber (Universität Freiburg). This research has been financially supported by the DFG through project EI 498/1-1 and the centre of excellence 595 *'Electrical Fatigue in Functional Materials'*.

* corresponding author, fax: +49-761-2036222, e-mail: ruediger.eichel@physchem.uni-freiburg.de

[1] M.J. Hoffmann, H. Kungl, Curr. Op. Solid State Mat. Sci. **8** (2004) 51
[2] P.V. Lambeck, G. H. Jonker, Ferroelectrics **22** (1978) 729
[3] R. Lohkämper, H. Neumann, G. Arlt, J Appl. Phys. **68** (1990) 4220
[4] R.-A. Eichel, P. Erhart, P. Träskelin, K. Albe, H. Kungl, M.J. Hoffmann, Phys. Rev. Lett. **100** (2008) 095504
[5] H. Meštrić, R.-A. Eichel, T. Kloss, K.-P. Dinse, So. Laubach, St. Laubach, P.C. Schmidt, Phys. Rev. B **71** (2005) 134109
[6] H. Meštrić, R.-A. Eichel, K.-P. Dinse, A. Ozarowski, J. van Tol, L.C. Brunel, H. Kungl, M.J. Hoffmann, K.A. Schönau, M. Knapp, Hartmut Fuess, Phys. Rev. B **73** (2006) 184105
[7] L.X. Zhang, E. Erdem, X. Ren, R.-A. Eichel, Appl. Phys. Lett. **93** (2008) 202901
[8] H.J. Kleebe, S. Lauterbach, L. Silvestroni, H. Kungl, M.J. Hoffmann, E. Erdem, R.-A. Eichel, Appl. Phys. Lett. **94** (2009) 142901
[9] R.-A. Eichel, H. Meštrić, H. Kungl, M.J. Hoffmann, Appl. Phys. Lett. **88** (2006) 122506
[10] X. Ren, Nature Mater. **3** (2004) 91
[11] Y.A. Genenko, Phys. Rev. B **78** (2008) 214103
[12] D.C. Lupascu, "*Fatigue in ferroelectric ceramics and related issues*" Springer, Heidelberg, (2004)
[13] N. Balke, D.C. Lupascu, T. Granzow, J. Rödel, J. Am. Ceram. Soc. **90** (2007) 1081-1087
[14] N. Balke, D. C. Lupascu, T. Granzow, J. Rödel, J. Am. Ceram. Soc. **90** (2007) 1088-1093
[15] S. Gottschalk, H. Hahn, S. Flege, A.G. Balogh, J. Appl. Phys. **104** (2008) 114106
[16] R.-A. Eichel, J. Electroceram. **19** (2007) 9-21
[17] R.-A. Eichel, J. Am. Ceram. Soc. **91** (2008) 691-701
[18] R.-A. Eichel, K.-P. Dinse, H. Kungl, M.J. Hoffmann, A. Ozarowski, J. van Tol, L.C. Brunel, Appl. Phys. A **80** (2005) 51-54
[19] H. Meštrić, R.-A. Eichel, K.-P. Dinse, A. Ozarowski, J. van Tol, L.C. Brunel, J. Appl. Phys. **96** (2004) 7440-7444
[20] R.-A. Eichel, H. Meštrić, K.P. Dinse, A. Ozarowski, J. van Tol, L.C. Brunel, H. Kungl, M.J. Hoffmann, Magn. Reson. Chem. **43** (2005) S166-S173
[21] E. Erdem, R. Böttcher, H.J. Gläsel, E. Hartmann, Magn. Reson. Chem. **43** (2005) 174182
[22] R.-A. Eichel, H. Kungl, M.J. Hoffmann, J. Appl. Phys. **95** (2004) 8092-8096
[23] R. Böttcher, W. Brunner, B. Milsch, G. Völkel, W. Windsch, S.T. Kirillov, Chem. Phys. Lett. **129** (1986) 546
[24] D.J. Newman, Adv. Phys. **20** (1971) 197

[25] A. Abragam, B. Bleaney: *Electron paramagnetic resonance of transition ions*, Clarendon Press, Oxford (1970)
[26] B.R. MaGarvey, J. Phys. Chem. **71** (1967) 51
[27] N.M. Atherton: *Principles of electron spin resonance*, Ellis Horwood, New York (1993)
[28] B. Bleaney, K.D. Bowers, M.H.L. Pryce, Proc. Roy Soc. A **228** (1955) 166
[29] W.L. Warren, B.A. Tuttle, F.C. Rong, G.J. Gerardi, E.H. Poindexter, J. Am. Ceram. Soc. **80** (1997) 680-684
[30] D.J. Keeble, Z. Li, M. Harmatz, J. Phys. Chem. Solids **57** (1996) 1513-1515
[31] R.E. Cohen, Nature **358** (1992) 136-138
[32] H. Miyazawa, E. Natori, S. Miyashita, T. Shimoda, F. Ishii, T. Oguchi, Jpn. J. Appl. Phys. **39** (2000) 5679-5682
[33] Y. Kuroiwa, S. Aoyagi, A. Sawada, J. Harada, E. Nishibori, M. Takata, M. Sakata, Phys. Rev. Lett. **87** (2001) 217601
[34] G.A. Rossetti, Brit. Ceram. Trans. **104** (2004) 83-87
[35] S. Aoyagi, Y. Kuroiwa, A. Sawada, H. Tanaka, J. Harada, E. Nishibori, M. Takata, M. Sakata, J. Phys. Soc. Jpn. **71** (2002) 2353-2356
[36] D. Kivelson, R. Neiman, J. Chem. Phys. **35** (1961) 149-155
[37] H. Imagawa, Phys. Status Solidi **30** (1968) 469
[38] H. Hosono, H. Kawazoe, T. Kanazawa, J. Non-Cryst. Solids **33** (1979) 103
[39] R.N. Schwartz, B.A. Wechsler, Phys. Rev. B **48** (1993) 7057-7069
[40] M.N. Lee, Y.C. Park, Bull. Kor. Chem. Soc. **16** (1995) 908-911
[41] H.T. Langhammer, T. Müller, R. Böttcher, H.P. Abicht, Solid State Sci. **5** (2003) 965-971
[42] R.-A. Eichel, A. Schweiger, J. Magn. Reson. **152** (2001) 276287
[43] H.R. Gersmann, J.D. Swalen, J. Chem. Phys. **36** (1962) 32213233
[44] A. Schweiger, H.H. Günthard, Chem. Phys. **32** (1978) 3561
[45] R.-A. Eichel, A. Schweiger, J. Chem. Phys. **115** (2001) 9126-9135
[46] A.H. Maki, B.R. McGarvey, J. Chem. Phys. **29** (1958) 3134
[47] S.K.S. Parashar, R.N.P. Choudhary, B.S. Murty, J. Appl. Phys. **94** (2003) 6091-6096
[48] P. Erhart, R.-A. Eichel, P. Träskelin, K. Albe, Phys. Rev. B **76** (2007) 174116
[49] U. Höchli, K.A. Müller, P. Wysling, Phys. Lett. **15** (1965) 5-6
[50] R.E. Coffman, J. Chem. Phys. **48** (1968) 609-618
[51] R.W. Reynolds, L.A. Boatner, M.M. Abraham, Y. Chen, Phys. Rev. B **10** (1974) 3802-3817
[52] A. Dick, E.R. Krausz, K.S. Hadler, C.J. Noble, P.L.W. Tregenna-Piggott, M.J. Riley, J. Phys. Chem. C **112** (2008) 14555-14562
[53] B.J. Hathaway, D.E. Billing, Corrd. Chem. Rev. **5** (1970) 143-207
[54] H.A. Buckmaster, Magn. Reson. Rev. **8** (1983) 283-409
[55] H.A. Buckmaster, Magn. Reson. Rev. **11** (1986) 81-204
[56] S.K. Misra, C. Wang, Magn. Reson. Rev. **14** (1990) 157-260
[57] R.M. Krishna, S.K. Gupta, Bull. Magn. Reson. **16** (1994) 239-291
[58] J. Peisach, E. Blumberg, Arch. Biochem. Biophys. **165** (1974) 691-708